

# GIFT: Unlocking Global Optimality in Post-Training via Finite-Temperature Gibbs Initialization

Zhengyang Zhao<sup>1,\*</sup>, Lu Ma<sup>1,\*</sup>, Yizhen Jiang<sup>1,2</sup>, Xiaochen Ma<sup>1</sup>, Zimo Meng<sup>1</sup>,  
 Chengyu Shen<sup>1</sup>, Lexiang Tang<sup>1</sup>, Haoze Sun<sup>2</sup>, Peng Pei<sup>2</sup>, Wentao Zhang<sup>1,†</sup>

<sup>1</sup>Peking University <sup>2</sup>Meituan

zhengyangzhao@stu.pku.edu.cn, maluqaq@163.com

## Abstract

The prevailing post-training paradigm for Large Reasoning Models (LRMs)—Supervised Fine-Tuning (SFT) followed by Reinforcement Learning (RL)—suffers from an intrinsic optimization mismatch: the rigid supervision inherent in SFT induces distributional collapse, thereby exhausting the exploration space necessary for subsequent RL. In this paper, we reformulate SFT within a unified post-training framework and propose Gibbs Initialization with Finite Temperature (GIFT). We characterize standard SFT as a degenerate zero-temperature limit that suppresses base priors. Conversely, GIFT incorporates supervision as a finite-temperature energy potential, establishing a distributional bridge that ensures objective consistency throughout the post-training pipeline. Our experiments demonstrate that GIFT significantly outperforms standard SFT and other competitive baselines when utilized for RL initialization, providing a mathematically principled pathway toward achieving global optimality in post-training. Our code is available at <https://github.com/zzy1127/GIFT>.

## 1 Introduction

The training pipeline for Large Reasoning Models (LRMs) has converged into a standard two-stage paradigm. First, Supervised Fine-Tuning (SFT) establishes fundamental reasoning capabilities by leveraging expert demonstrations (Chung et al., 2022; Ouyang et al., 2022; Touvron et al., 2023). Second, Reinforcement Learning (RL) encourages the model to explore self-generated reasoning paths, allowing it to optimize for correctness beyond the constraints of static datasets (Shao et al., 2024a; Yu et al., 2025; Rafailov et al., 2024; Schulman et al., 2017). This hierarchical approach

underpins current state-of-the-art reasoning systems (DeepSeek-AI et al., 2025b; Yang et al., 2025; Nvidia et al., 2024).

However, a fundamental theoretical discrepancy persists between these two phases. While SFT typically minimizes cross-entropy loss to imitate expert tokens, RL maximizes expected rewards through environmental exploration. Standard SFT aggressively suppresses the probability mass of non-target tokens, thereby forcing the policy distribution to collapse onto deterministic data points (Wu et al., 2025). This phenomenon, characterized as distributional collapse, erodes the structural priors inherited from pre-training and severely restricts the subsequent exploration space (Li et al., 2025). Consequently, as the model transitions to the RL stage, it encounters a critical bottleneck: the stochastic diversity required to discover high-reward trajectories has been effectively extinguished by the rigid supervision of the preceding SFT phase (Gudibande et al., 2023; Kang et al., 2025).

Previous research has attempted to mitigate this issue by heuristically tuning data mixtures and inter-stage scheduling (Kang et al., 2025; Liu et al., 2025b), or by modifying the SFT objective to implicitly incorporate RL properties (Zhu et al., 2025b; Wu et al., 2025; Du et al., 2025; Rafailov et al., 2024). In contrast to these methods, we do not attempt to bypass the RL stage or rely on heuristic adjustments; instead, we aim to establish a mathematically optimal coupling between the two phases. We posit that SFT should not be treated as an isolated imitation task but rather as a rigorously defined initialization for subsequent RL within a unified global post-training framework.

Based on this principle, we derive the optimal initialization for subsequent RL within a unified post-training framework and propose **Gibbs Initialization with Finite Temperature (GIFT)** to realize this objective. GIFT ensures that while the model is trained to prioritize expert trajectories, it

\*Equal contribution.

†Corresponding author.

preserves the structural knowledge and inherent capabilities of the base model, offering a thermodynamic resolution to the alignment-exploration trade-off. Within our principled framework, standard SFT is characterized as a degenerate zero-temperature limit that induces a rigid distributional collapse onto the expert data. In contrast, GIFT maintains a finite temperature, enabling the model to incorporate expert supervision as a continuous re-weighting of the base distribution rather than a destructive overwrite.

Empirically, we conduct SFT followed by RL on a subset of the DeepMath-103k dataset (He et al., 2025). Experimental results demonstrate that GIFT significantly outperforms standard SFT and other robust SFT variants when utilized as an initialization policy for RL across diverse mathematical reasoning benchmarks and out-of-distribution (OOD) tasks. Furthermore, our geometric and distributional analyses reveal that GIFT maintains objective consistency throughout the two-stage post-training process. By preserving the exploration landscape, GIFT facilitates accelerated convergence and superior asymptotic performance during the subsequent RL stage, effectively unlocking the model’s full reasoning potential.

The contributions of this work are twofold, spanning theoretical and practical dimensions. Theoretically, we formally establish a framework for post-training global optimality and identify the optimal initial policy for the subsequent RL as a Gibbs distribution. We further demonstrate that standard SFT is a degenerate zero-temperature limit of this optimal initialization. Practically, we propose GIFT to realize this initialization. Extensive experiments demonstrate that GIFT significantly outperforms robust SFT baselines on reasoning and OOD benchmarks, while maintaining superior objective consistency throughout the two-stage post-training pipeline.

## 2 Related Work

**Post-training for Reasoning: SFT-then-RL Paradigm.** Post-training for reasoning LLMs typically follows a two-stage paradigm: Supervised Fine-Tuning (SFT) and Reinforcement Learning with Verifiable Rewards (RLVR) (DeepSeek-AI et al., 2025a; Team et al., 2025; Liu et al., 2025b). SFT acts as a "cold-start" phase, establishing a strong initial policy by training on high-quality reasoning chains. Subsequently, RLVR enhances

problem-solving capabilities by allowing the model to explore the solution space beyond the SFT data, discovering novel and more robust reasoning paths. However, this transition is impeded by an intrinsic optimization conflict (Ouyang et al., 2022; Touvron et al., 2023). Specifically, SFT typically compels the model to fit deterministic one-hot labels, which aggressively suppresses the probability mass of alternative tokens. In contrast, RL necessitates a high-entropy policy distribution to facilitate exploration and the discovery of high-reward trajectories (Chen et al., 2025a; Zhang et al., 2024; Kumar et al., 2022). This mismatch often causes SFT to overfit specific patterns and induce a collapse of the probability manifold, thereby stifling the exploration capacity required for the subsequent RL stage (Kang et al., 2025; Vattikonda et al., 2025).

**Improve the generalizability of SFT.** To mitigate the distributional degradation inherent in SFT, various studies have focused on refining its optimization objectives. One prominent research direction focuses on modifying the training loss. (Li et al., 2025) proposes dynamic objectives that adapt to model capabilities, while DFT (Wu et al., 2025) re-weights SFT loss based on prediction probabilities. ASFT (Zhu et al., 2025a) observes that such weighting can induce distribution drift and introduces a KL-divergence anchoring term as a solution. (Zhu et al., 2025b) applies a PPO-style clipping mechanism to prune tokens with excessive probability ratios. Another research avenue attempts to refine loss computation via critical token selection. (Wang et al., 2025; Jiang et al., 2025) demonstrate that high-entropy tokens act as pivotal decision points in reasoning. CFT (Ruan et al., 2025) employs counterfactual perturbations to identify and isolate loss calculation to essential reasoning tokens. Despite these efforts, the distributional damage caused by SFT remains an unaddressed challenge in the perspective of full post-training.

**Unified Paradigms of SFT and RL.** While the SFT-then-RL paradigm remains dominant, recent research has sought to bridge these two stages. Recent efforts include iterating or interleaving SFT and RL (Ma et al., 2025), gradually shifting from SFT to RL (Zhang et al., 2025), or unifying their objectives into a single framework (Yan et al., 2025; Ming et al., 2025; Liu et al., 2025a; Chen et al., 2025b). Despite their potential, these unified approaches introduce substantial complexity and have yet to supersede the SFT-then-RL pipeline, which

remains the industry standard due to its empirical robustness. In contrast, our work operates within this SFT-then-RL paradigm, proposing a novel fine-tuning method designed to optimize performance across the entire post-training pipeline.

### 3 Method

In this section, we propose a novel training approach termed **Gibbs Initialization with Finite Temperature (GIFT)**. GIFT is grounded in the theoretical framework of unifying the two-stage post-training process—namely, SFT and RL—into a single global optimization objective. Leveraging the hypothesis of global optimality in post-training, we derive the optimal initialization: a Gibbs distribution that serves as a mathematically principled starting point for subsequent RL. Finally, we present a token-level implementation that transforms this theoretical objective into a practical loss function for LLM training.

#### 3.1 Preliminaries

**Supervised Fine-Tuning.** Starting with a pre-trained base model  $\pi_{\text{base}}$  and a curated dataset of high-quality demonstrations  $\mathcal{D} = \{(x, y^*)\}$ , SFT optimizes the model parameters  $\theta$  to maximize the log-likelihood of the target sequences. The objective is typically formulated as a cross-entropy loss:

$$\begin{aligned} \mathcal{L}_{\text{SFT}}(\theta) &= -\mathbb{E}_{(x, y^*) \sim \mathcal{D}} \log \pi_\theta(y^* | x) \\ &= -\mathbb{E}_{(x, y^*) \sim \mathcal{D}} \sum_{t=1}^{|y^*|} [\log \pi_\theta(y_t^* | x, y_{<t}^*)]. \end{aligned} \quad (1)$$

By minimizing this negative log-likelihood, the model learns to imitate the distribution of the expert data, providing a specialized foundation for subsequent alignment or reasoning-based stages.

**Reinforcement Learning with Verifiable Rewards.** Following SFT, the model  $\pi_{\text{sft}}$  is further refined using RL algorithms—such as PPO (Schulman et al., 2017) or GRPO (Shao et al., 2024b)—to maximize an objective  $J_{\text{RL}}(\theta)$  based on a reward  $R(x, y)$ :

$$J_{\text{RL}}(\theta) = \mathbb{E}_{x \sim \mathcal{D}, y \sim \pi_\theta} \left[ R(x, y) - \frac{1}{\eta} D_{\text{KL}}(\pi_\theta \| \pi_{\text{sft}}) \right] \quad (2)$$

where  $\eta > 0$  is the inverse temperature parameter governing the strength of the Kullback–Leibler (KL) regularization. This penalty ensures the optimized model  $\pi_\theta$  does not deviate excessively from

the initial  $\pi_{\text{sft}}$ . This stage is critical for incentivizing advanced reasoning capabilities in LLMs, aiming to achieve superior performance that transcends the inherent limitations of static SFT datasets.

#### 3.2 The Global Optimum of Post-Training

A critical limitation of the prevailing post-training paradigm (i.e. SFT followed by RL) is that these two stages are predominantly treated as disjoint optimization tasks. While recent studies have attempted to bridge this gap by coordinating training data or scheduling steps (Vattikonda et al., 2025; Kang et al., 2025), the underlying objective functions remain fundamentally uncoupled. We hypothesize that for post-training to reach its full potential, SFT should not be viewed merely as a preliminary task, but as an explicit initialization phase mathematically aligned with the subsequent RL objective. By unifying these stages, we aim to converge toward a singular, comprehensive goal: the **global optimum** of post-training.

We define post-training objective as identifying an optimal policy  $\pi_{\text{global}}^*$  that maximizes expected rewards while remaining anchored to the foundational knowledge of the base model  $\pi_{\text{base}}$ . Formally, this global objective is formulated as:

$$\begin{aligned} \pi_{\text{global}}^*(\cdot | x) &= \arg \max_{\pi} \mathbb{E}_{x \sim \mathcal{D}, y \sim \pi(\cdot | x)} [ \\ &\quad R(x, y) - \frac{1}{\eta} D_{\text{KL}}(\pi(\cdot | x) \| \pi_{\text{base}}(\cdot | x))]. \end{aligned} \quad (3)$$

Following the derivation principles of previous work (Rafailov et al., 2024; Peters et al., 2010), the closed-form solution to Eq. 3 is given by the Gibbs distribution:

$$\pi_{\text{global}}^*(y | x) = \frac{1}{Z_{\text{base}}(x)} \pi_{\text{base}}(y | x) e^{\eta R(x, y)} \quad (4)$$

where  $Z_{\text{base}}(x) = \sum_y \pi_{\text{base}}(y | x) e^{\eta R(x, y)}$  is the partition function. This distribution represents the information-theoretically optimal balance between maximizing external rewards and preserving the structural priors of the base model. While one could theoretically attempt to optimize  $\pi_{\text{base}}$  toward  $\pi_{\text{global}}^*$  directly via RL, this approach is computationally intractable for LLMs. In practice, direct sampling during RL often yields vanishingly sparse rewards, which prevents the optimization process from converging.

---

**Algorithm 1** GIFT: Gibbs Initialization with Finite Temperature

---

- 1: **Input:** Dataset  $\mathcal{D}$ , Initialized model  $\pi_\theta$ , Base model  $\pi_{\text{base}}$
- 2: **Hyper:** Inverse temperature gain  $\beta$ , Learning rate  $\alpha$
- 3: Initialize:  $\theta \leftarrow \theta_{\text{base}}$
- 4: **while** not converged **do**
- 5:   Sample a batch of sequences  $(x, y^*) \sim \mathcal{D}$
- 6:   Forward pass with base model to get logits  $z_{\text{base}}$  for all steps  $t$ .
- 7:   Compute log-probabilities:  $\log p_{\text{ref}}(v|x, y_{<t}^*) = \text{LogSoftmax}(z_{\text{base}})_v$
- 8:   For each timestep  $t$ , construct the advantage-adjusted target logits  $\hat{z}$ :

$$\hat{z}_{t,k} = \begin{cases} \log p_{\text{ref}}(k|x, y_{<t}^*) + \beta & \text{if } k = y_t^* \\ \log p_{\text{ref}}(k|x, y_{<t}^*) & \text{if } k \neq y_t^* \end{cases}$$

- 9:   Compute target distribution:  $\pi_{\text{sft}}^*(\cdot | x, y_{<t}^*) = \text{Softmax}(\hat{z}_t)$
- 10:   Update  $\theta$  by minimizing the cross-entropy loss against soft targets:

$$\mathcal{L}(\theta) = -\frac{1}{B} \sum_{i=1}^B \sum_{t=1}^{|y^*|} \sum_{v \in \mathcal{V}} \pi_{\text{sft}}^*(v | x, y_{<t}^*) \log \pi_\theta(v | x, y_{<t}^*)$$

- 11:    $\theta \leftarrow \theta - \alpha \nabla_\theta \mathcal{L}(\theta)$

- 12: **end while**

- 13: **return**  $\theta$

---

### 3.3 Deriving the Optimal Initial Policy

To ensure the two-stage post-training process achieves the global optimum, the convergence point of the RL stage must coincide with  $\pi_{\text{global}}^*$ . Typically, an RL stage initialized from a policy  $\pi_{\text{sft}}$  converges to:

$$\pi_{\text{stage2}}^*(y|x) = \frac{1}{Z_{\text{sft}}(x)} \pi_{\text{sft}}(y|x) \cdot e^{\lambda R(x,y)}, \quad (5)$$

where  $\lambda > 0$  governs the strength of the KL regularization. By enforcing the condition  $\pi_{\text{stage2}}^* \equiv \pi_{\text{global}}^*$  and substituting Eq. 4 and Eq. 5, we obtain:

$$\frac{\pi_{\text{sft}}(y|x) \cdot e^{\lambda R(x,y)}}{Z_{\text{sft}}(x)} = \frac{\pi_{\text{base}}(y|x) \cdot e^{\eta R(x,y)}}{Z_{\text{base}}(x)} \quad (6)$$

Solving for  $\pi_{\text{sft}}$ , we derive the optimal initial policy for the subsequent RL stage:

$$\pi_{\text{sft}}^*(y|x) = \frac{1}{Z(x)} \pi_{\text{base}}(y|x) \cdot e^{\beta R(x,y)}, \quad (7)$$

where  $\beta = \eta - \lambda$  represents finite inverse temperature for this Gibbs distribution. This result provides a thermodynamic critique of current paradigms: standard SFT effectively assumes  $\beta \rightarrow \infty$  (a zero-temperature limit), forcing the policy to collapse

onto a Dirac distribution. In contrast, GIFT maintains a finite  $\beta$ , acting as a reward-weighted scaling that amplifies high-quality sequences while preserving the structural priors of the base model.

To implement this sequence-level objective autoregressively, we apply a token-level decomposition under sparse reward assumptions (see Appendix B), yielding:

$$\pi_{\text{sft}}^*(y_t|y_{<t}, x) \propto \pi_{\text{base}}(y_t|y_{<t}, x) \cdot e^{\beta \cdot \mathbb{I}(y_t = y_t^*)}. \quad (8)$$

This formulation translates the global objective into a practical soft-target mechanism. By augmenting the ground-truth logits with the scalar  $\beta$ , GIFT aligns the model with the expert trajectory while avoiding the "freezing" effect characteristic of one-hot supervision, thereby preserving the exploration capacity essential for the subsequent RL stage.

### 3.4 Proposed Algorithm: GIFT

To realize this token-level optimal initialization, we minimize the KL divergence between our theoretically optimal target distribution  $\pi_{\text{sft}}^*$  and the parameterized model  $\pi_\theta$ :

$$\mathcal{L}(\theta) = -\mathbb{E}_{(x,y^*) \sim \mathcal{D}} [D_{\text{KL}}(\pi_{\text{sft}}^*(y^*|x) \parallel \pi_\theta(y^*|x))] \quad (9)$$

By expanding the KL divergence and isolating the cross-entropy term (since the entropy of the target distribution is constant with respect to  $\theta$ ), we obtain the following optimization objective:

$$\mathcal{L}(\theta) = -\mathbb{E}_{(x, y^*) \sim \mathcal{D}} \left[ \sum_{t=1}^{|y^*|} \sum_{y_t \in \mathcal{V}} \pi_{\text{sft}}^*(y_t | x, y_{t-1}^*) \log \pi_\theta(y_t | x, y_{t-1}^*) \right] \quad (10)$$

GIFT ensures that while the model is incentivized to prioritize the expert trajectory, it retains the structural knowledge and capabilities of the base model. By preventing premature policy collapse, this approach maintains the exploration capacity essential for the subsequent RL phase. The complete procedure is detailed in Algorithm 1.

## 4 Experiments

### 4.1 Experimental setup

**Datasets.** We utilize **DeepMath-103k** (He et al., 2025), a large-scale mathematical dataset specifically curated for high-difficulty reasoning tasks. It undergoes a rigorous decontamination process against multiple public benchmarks and provides verifiable ground-truth answers to facilitate rule-based rewards. Each problem is accompanied by high-quality solutions generated by DeepSeek-R1 (DeepSeek-AI et al., 2025a). From the full DeepMath-103k corpus, we randomly sample three disjoint subsets for our experiments: 10,000 samples for SFT, 10,000 samples for RL, and 1,000 samples as a validation set to monitor convergence during the SFT stage.

**Evaluation.** To comprehensively assess the mathematical reasoning capabilities, we employ a suite of five widely adopted benchmarks: **GSM8K** (Cobbe et al., 2021) for grade-school math; **Math500** (Hendrycks et al., 2021), a rigorous subset of the MATH dataset; **Olympiad-Bench** (He et al., 2024) for competition-level problems; and **AIME24 & AIME25** to test performance on high-difficulty mathematics competitions. Furthermore, to verify generalizability, we evaluate on four general benchmarks: **GPQA** (Rein et al., 2023) for graduate-level reasoning, **MMLU-Pro** (Wang et al., 2024) and **MMLU-Redux** (Gema et al., 2025) for massive multitask language understanding, and **ARC-Challenge** (Clark et al., 2018) for common-sense reasoning. All evaluations are conducted by VeRL (Sheng et al., 2024) with the vLLM backend. We set the maximum response

length to 8,192 tokens and temperature  $T = 0.6$  to evaluate the robustness of the policy.

**Baselines and Implementation.** We evaluate various initialization strategies on two backbone models, Qwen2.5-7B and Llama-3.1-8B, categorizing baselines into three groups: (1) **Direct SFT/RL**, which includes standard SFT on the base model and applying RL directly without prior fine-tuning; (2) **Unified Paradigms**, featuring recent methods like LUFFY (Yan et al., 2025) and ReLIFT (Ma et al., 2025); and (3) **SFT-then-RL**, where we compare our proposed GIFT against several initialization variants, including Standard SFT, SFT+Entropy ( $\lambda = 0.01$ ), and density-based or proximal methods such as DFT (Wu et al., 2025), ASFT (Zhu et al., 2025a), and PSFT (Zhu et al., 2025b). Notably, we omit the results of Unified Paradigms on Llama-3.1-8B due to their consistently poor performance on this weaker backbone. For Llama-3.1-8B, a uniform distribution smoothing term was added to maintain training stability (see Appendix C). In the subsequent RL stage, we uniformly employ GRPO (Shao et al., 2024a) via the VeRL framework. Training is configured with a group size of  $G = 8$ , a learning rate of  $1 \times 10^{-6}$ , a PPO clip ratio of 0.2, and a maximum length of 8,192 tokens for long chain-of-thought reasoning. All models are trained for one epoch on  $8 \times$ NVIDIA H200 GPUs. Detailed hyperparameters are provided in Appendix E.

### 4.2 Main Results

We demonstrate the excellent performance of GIFT initialization from three aspects: significant improvements in mathematical reasoning tasks, robust OOD generalization, and superior exploration potential as evidenced by pass@k scaling prior the RL training.

**Mathematical Reasoning Performance.** As shown in Table 1, GIFT consistently achieves best performance across all initialization strategies on both Qwen2.5-7B and Llama-3.1-8B. On Qwen2.5-7B, GIFT attains an average pass@1 of 52.43%, surpassing not only strong SFT variants like PSFT (50.76%) but also complex unified paradigms such as LUFFY (50.15%). Notably, on the challenging AIME benchmark, GIFT yields a substantial gain of nearly 10% over Standard SFT (13.33%  $\rightarrow$  23.33%). On the weaker Llama-3.1-8B, GIFT similarly leads with an impressive 35.60%, outperforming Standard SFT (29.20%) and PSFT (30.21%) by significant margins. In contrast, while simple

Table 1: Average pass@1 performance of different initialization strategies for subsequent RL on five mathematical reasoning benchmarks. The best performance of each strategy across benchmarks is bold.

Method Class	Strategy	GSM8K	OlympiadBench	AIME24	AIME25	MATH500	Average
<b><i>Qwen2.5-7B</i></b>							
<i>Direct SFT/RL</i>	Direct SFT	90.25	39.26	15.00	16.66	74.30	47.09
	Direct RL	90.50	40.64	12.22	6.67	77.13	45.43
<i>Unified Paradigms</i>	LUFFY	<b>92.70</b>	47.04	15.00	15.83	80.20	50.15
	ReLIFT	91.84	44.96	14.06	17.50	79.72	49.62
<i>SFT-then-RL</i>	SFT	91.79	44.69	13.33	14.44	78.67	48.58
	SFT + Entropy	90.90	45.56	18.33	11.67	79.90	49.27
	DFT	86.50	33.28	6.67	8.89	65.87	40.24
	ASFT	90.65	38.42	12.22	7.78	74.07	44.62
	PSFT	91.94	<b>48.04</b>	15.83	16.67	81.33	50.76
	<b>GIFT</b>	92.06	46.96	<b>23.33</b>	<b>17.78</b>	<b>82.00</b>	<b>52.43</b>
<b><i>Llama3.1-8B</i></b>							
<i>Direct SFT/RL</i>	Direct SFT	75.59	14.23	6.67	10.00	39.50	29.20
	Direct RL	49.18	5.29	10.00	<b>16.67</b>	22.27	20.68
<i>SFT-then-RL</i>	SFT	73.39	12.15	16.67	6.67	39.20	29.62
	SFT + Entropy	70.24	11.63	<b>23.33</b>	13.33	36.30	30.97
	DFT	64.75	7.80	13.33	3.33	29.47	23.74
	ASFT	60.78	7.56	13.33	3.33	24.33	21.87
	PSFT	74.53	13.78	16.67	6.67	39.40	30.21
	<b>GIFT</b>	<b>81.33</b>	<b>15.56</b>	<b>23.33</b>	13.33	<b>44.45</b>	<b>35.60</b>

regularization via SFT + Entropy yields moderate improvements, baselines such as DFT and ASFT exhibit severe degradation. These results suggest that while other methods suffer from optimization instability on models with limited intrinsic capabilities, GIFT serves as a robust stabilizer, effectively unlocking performance gains where baselines fail.

**Generalization Capabilities.** Table 2 details the OOD performance across different initialization strategies. GIFT demonstrates robust generalization capabilities, effectively preserving the base model’s knowledge against the distributional collapse typical of Standard SFT. On Qwen2.5-7B, GIFT achieves an average score of 64.10%, significantly outperforming Standard SFT (59.78%) and maintaining performance parity with complex Unified Paradigms like ReLIFT (64.55%). On Llama-3.1-8B, GIFT secures the highest average performance (55.24%), surpassing all baselines. These results confirm that by maintaining a finite temperature, GIFT successfully retains the structural priors essential for broad generalization, whereas standard zero-temperature SFT is prone to overfitting.

**Exploration Potential.** We evaluate the exploration capability of the initialized policies by comparing pass@k performance ( $k \in \{1, 2, 4, 8\}$ ) prior to RL. As illustrated in Figure 1, GIFT demonstrates superior scaling with sample size compared

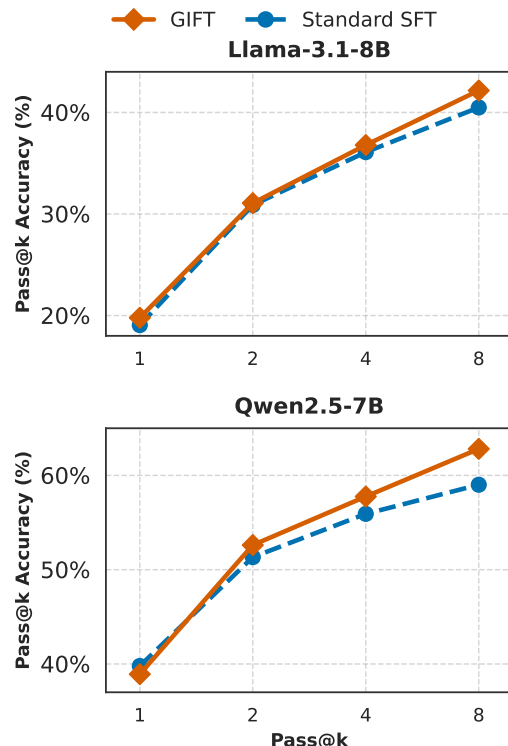


Figure 1: **Pass@k performance comparison.** We compare the average accuracy of GIFT versus Standard SFT across varying sample counts ( $k$ ) prior to RL training.

Table 2: Average pass@1 performance of different initialization strategies for subsequent RL on four out-of-distribution benchmarks. The best performance of each strategy across benchmarks is bold.

Method Class	Strategy	GPQA	MMLU-Redux	ARC-Challenge	MMLU-Pro	Average
<i>Qwen2.5-7B</i>						
<i>Direct SFT/RL</i>	Direct SFT	19.70	69.03	82.68	50.23	55.41
	Direct RL	32.32	70.50	73.85	54.33	57.75
<i>Unified Paradigms</i>	LUFFY	34.85	73.30	89.85	<b>59.08</b>	64.27
	ReLIFT	37.88	73.67	<b>89.85</b>	56.82	<b>64.55</b>
<i>SFT-then-RL</i>	SFT	27.78	71.13	85.54	54.67	59.78
	SFT + Entropy	33.33	72.20	87.29	55.60	62.11
	DFT	17.17	57.77	84.85	39.75	49.89
	ASFT	25.25	68.27	86.90	49.98	57.60
	PSFT	34.34	<b>73.79</b>	87.77	59.05	63.74
	<b>GIFT</b>	<b>39.09</b>	73.27	88.01	56.01	64.10
<i>Llama3.1-8B</i>						
<i>Direct SFT/RL</i>	Direct SFT	21.21	61.50	77.82	40.05	50.14
	Direct RL	23.74	52.13	64.59	29.65	42.53
<i>SFT-then-RL</i>	SFT	23.74	55.97	74.49	33.67	46.97
	SFT + Entropy	27.78	<b>63.37</b>	80.25	41.87	53.32
	DFT	24.24	54.27	71.46	35.59	46.39
	ASFT	13.13	47.23	66.42	29.40	39.05
	PSFT	12.12	44.67	46.54	30.14	33.37
	<b>GIFT</b>	<b>30.81</b>	63.17	<b>82.94</b>	<b>44.05</b>	<b>55.24</b>

to Standard SFT. While standard SFT exhibits competitive pass@1 performance (e.g., 39.79% vs. 38.92% on Qwen2.5-7B), its gains diminish as  $k$  increases, indicating potential mode collapse. In contrast, GIFT’s advantage expands significantly at higher  $k$ ; notably, on Qwen2.5-7B, GIFT reverses the initial gap to achieve a substantial +3.8% lead at pass@8 (62.81% vs. 59.01%). This trend confirms that GIFT preserves a more diverse output distribution, providing a broader and more effective search space for subsequent reinforcement learning.

### 4.3 Analysis of Inverse Temperature

The inverse temperature  $\beta$  regulates the trade-off between exploiting expert data and exploring the base model priors. By varying  $\beta$ , we analyze the sensitivity of post-RL performance on mathematical reasoning benchmarks to the initialization temperature. As illustrated in Figure 2, performance improves and reaches an optimal range as the inverse temperature increases, before subsequently degrading toward the standard SFT baseline. This trend confirms that neither the under-constrained base model ( $\beta \rightarrow 0$ ) nor the over-constrained SFT limit ( $\beta \rightarrow \infty$ ) is optimal. Standard SFT forces a zero-temperature collapse, inhibiting the ability required for RL exploration. GIFT identifies an optimal finite window that varies according to the

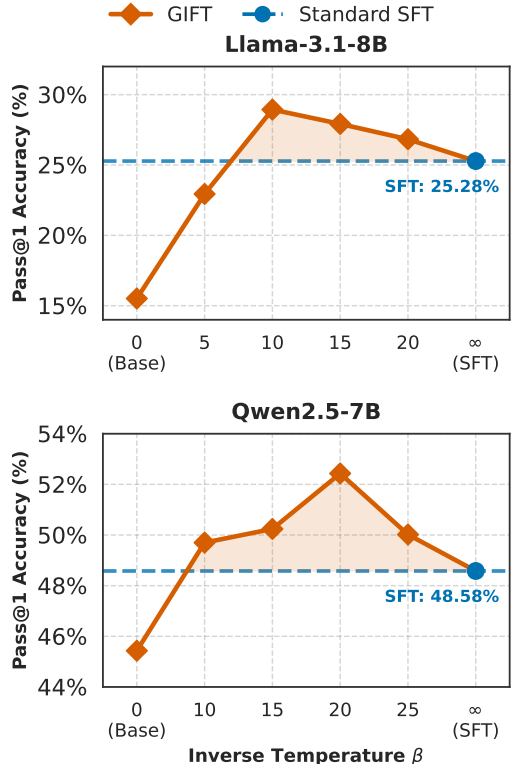


Figure 2: **Impact of inverse temperature  $\beta$  on RL performance.** Average accuracy on math benchmarks peaks at finite  $\beta$  for both models, surpassing the standard SFT baseline (dashed line).

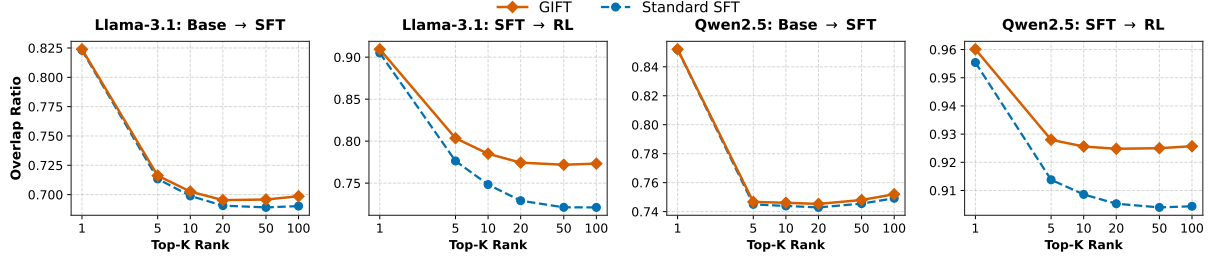


Figure 3: **Top- $K$  Token Overlap Analysis.** Results for Llama-3.1-8B (Left) and Qwen2.5-7B (Right). GIFT exhibits consistently higher token overlap than the SFT baseline.

Table 3: **Consistency Metrics across Training Stages.**

Method	Stage 1 Base $\rightarrow$ SFT			Stage 2 SFT $\rightarrow$ RL		
	Cos $\uparrow$	L2 $\downarrow$	KL $\downarrow$	Cos $\uparrow$	L2 $\downarrow$	KL $\downarrow$
<i>Llama-3.1-8B</i>						
Std. SFT	0.8112	87.33	<b>0.5893</b>	0.9310	53.85	0.2316
GIFT	<b>0.8207</b>	<b>85.05</b>	0.5909	<b>0.9422</b>	<b>49.08</b>	<b>0.2010</b>
<i>Qwen2.5-7B</i>						
Std. SFT	0.9201	117.18	0.3995	0.9764	62.61	0.0426
GIFT	<b>0.9253</b>	<b>113.95</b>	<b>0.3907</b>	<b>0.9869</b>	<b>47.34</b>	<b>0.0327</b>

underlying backbone; for instance, Qwen2.5-7B achieves peak performance at a higher inverse temperature ( $\beta \approx 20$ ) than Llama-3.1-8B ( $\beta \approx 10$ ). Consequently, distinct architectures require tailored initialization temperatures to account for their varying sensitivities to supervision pressure and to maximize their reasoning potential during RL.

#### 4.4 Geometric and Distributional Consistency

To validate whether the finite-temperature initialization fosters a more continuous and stable optimization trajectory during post-training, we analyze the geometric and distributional properties of the model updates. We evaluate the model’s representational and distributional shifts across two sequential stages: (1) the transition from the base model to the initialized policy (*Base  $\rightarrow$  SFT*), and (2) the subsequent evolution from the initialized policy to the final RL model (*SFT  $\rightarrow$  RL*). We quantify geometric consistency using cosine similarity and L2 distance of the last transformer layer, while measuring distributional consistency via KL divergence and Top- $K$  token overlap.

**Geometric Consistency.** As reported in Table 3, GIFT significantly enhances geometric consistency throughout the post-training process. GIFT consistently exhibits higher cosine similarity and lower L2 distance compared to standard SFT across stages and models. This indicates that GIFT effectively absorbs task-specific supervision while

adhering to the base model’s semantic manifold, reducing the destructive parameter updates caused by standard SFT, thereby providing a more efficient exploration for the subsequent RL stage.

**Distributional Consistency.** As shown in Table 3, GIFT reduces KL divergence across the entire post-training pipeline in most cases. Complementing this, the top- $k$  token overlap analysis in Figure 3 reveals that GIFT mitigates the drastic distributional shifts characteristic of standard SFT. Moreover, we can observe that the preservation of base priors during SFT stage is effectively leveraged in the subsequent RL stage, manifesting as higher top- $k$  overlap that facilitates more efficient exploration. These metrics confirm that GIFT preserves distributional consistency throughout initialization and RL, validating that finite-temperature updates foster superior performance by maintaining optimization coherence.

## 5 Conclusion

In this work, we establish a unified framework for the global post-training objective and identify the zero-temperature collapse induced by standard SFT. Through theoretical derivation, we propose Gibbs Initialization with Finite Temperature (GIFT) as the theoretically optimal initialization strategy for RL. Extensive experiments validate its effectiveness across mathematical reasoning and out-of-distribution tasks. Further analysis demonstrates that GIFT achieves superior performance, accompanied by well-preserved geometric and distributional consistency throughout post-training. Our work provides a global theoretical perspective for the traditional two-stage paradigm and offers a principled pathway toward constructing more robust and generalizable reasoning systems.

## 6 Limitations

Currently, the inverse temperature  $\beta$  is treated as a fixed hyperparameter determined by the underlying model characteristics. While this formulation provides a stable initialization, it does not dynamically account for the varying difficulty of individual samples or the evolving confidence of the policy. Developing an adaptive approach to implicitly adjust  $\beta$  during training—potentially eliminating the need for pre-defined configuration—remains a promising direction to further enhance the framework’s robustness and ease of use.

## References

Howard Chen, Noam Razin, Karthik Narasimhan, and Danqi Chen. 2025a. *Retaining by doing: The role of on-policy data in mitigating forgetting*. *Preprint*, arXiv:2510.18874.

Huayu Chen, Kaiwen Zheng, Qinsheng Zhang, Ganqu Cui, Yin Cui, Haotian Ye, Tsung-Yi Lin, Ming-Yu Liu, Jun Zhu, and Haoxiang Wang. 2025b. *Bridging supervised learning and reinforcement learning in math reasoning*. *Preprint*, arXiv:2505.18116.

Hyung Won Chung, Le Hou, Shayne Longpre, Barret Zoph, Yi Tay, William Fedus, Yunxuan Li, Xuezhi Wang, Mostafa Dehghani, Siddhartha Brahma, Albert Webson, Shixiang Shane Gu, Zhuyun Dai, Mirac Suzgun, Xinyun Chen, Aakanksha Chowdhery, Alex Castro-Ros, Marie Pellat, Kevin Robinson, and 16 others. 2022. *Scaling instruction-finetuned language models*. *Preprint*, arXiv:2210.11416.

Peter Clark, Isaac Cowhey, Oren Etzioni, Tushar Khot, Ashish Sabharwal, Carissa Schoenick, and Oyvind Tafjord. 2018. *Think you have solved question answering? try arc, the ai2 reasoning challenge*. *Preprint*, arXiv:1803.05457.

Karl Cobbe, Vineet Kosaraju, Mohammad Bavarian, Mark Chen, Heewoo Jun, Lukasz Kaiser, Matthias Plappert, Jerry Tworek, Jacob Hilton, Reiichiro Nakano, Christopher Hesse, and John Schulman. 2021. *Training verifiers to solve math word problems*. *Preprint*, arXiv:2110.14168.

DeepSeek-AI, Daya Guo, Dejian Yang, Haowei Zhang, Junxiao Song, Ruoyu Zhang, Runxin Xu, Qihao Zhu, Shirong Ma, Peiyi Wang, Xiao Bi, Xiaokang Zhang, Xingkai Yu, Yu Wu, Z. F. Wu, Zhibin Gou, Zhi-hong Shao, Zhuoshu Li, Ziyi Gao, and 181 others. 2025a. *Deepseek-r1: Incentivizing reasoning capability in llms via reinforcement learning*. *Preprint*, arXiv:2501.12948.

DeepSeek-AI, Aixin Liu, Bei Feng, Bing Xue, Bingxuan Wang, Bochao Wu, Chengda Lu, Chenggang Zhao, Chengqi Deng, Chenyu Zhang, Chong Ruan, Damai Dai, Daya Guo, Dejian Yang, Deli Chen, Dongjie Ji, Erhang Li, Fangyun Lin, Fucong Dai, and 181 others. 2025b. *Deepseek-v3 technical report*. *Preprint*, arXiv:2412.19437.

Yuhao Du, Zhuo Li, Pengyu Cheng, Zhihong Chen, Yuejiao Xie, Xiang Wan, and Anningzhe Gao. 2025. *Simplify rlhf as reward-weighted sft: A variational method*. *Preprint*, arXiv:2502.11026.

Aryo Pradipta Gema, Joshua Ong Jun Leang, Giwon Hong, Alessio Devoto, Alberto Carlo Maria Mancino, Rohit Saxena, Xuanli He, Yu Zhao, Xiaotang Du, Mohammad Reza Ghasemi Madani, Claire Barale, Robert McHardy, Joshua Harris, Jean Kaddour, Emile van Krieken, and Pasquale Minciervini. 2025. *Are we done with mmlu?* *Preprint*, arXiv:2406.04127.

Arnav Gudibande, Eric Wallace, Charlie Snell, Xinyang Geng, Hao Liu, Pieter Abbeel, Sergey Levine, and Dawn Song. 2023. *The false promise of imitating proprietary llms*. *Preprint*, arXiv:2305.15717.

Chaoqun He, Renjie Luo, Yuzhuo Bai, Shengding Hu, Zhen Leng Thai, Junhao Shen, Jinyi Hu, Xu Han, Yujie Huang, Yuxiang Zhang, Jie Liu, Lei Qi, Zhiyuan Liu, and Maosong Sun. 2024. *Olympiadbench: A challenging benchmark for promoting agi with olympiad-level bilingual multimodal scientific problems*. *Preprint*, arXiv:2402.14008.

Zhiwei He, Tian Liang, Jiahao Xu, Qizhi Liu, Xingyu Chen, Yue Wang, Linfeng Song, Dian Yu, Zhenwen Liang, Wenxuan Wang, and 1 others. 2025. *Deepmath-103k: A large-scale, challenging, decontaminated, and verifiable mathematical dataset for advancing reasoning*. *arXiv preprint arXiv:2504.11456*.

Dan Hendrycks, Collin Burns, Saurav Kadavath, Akul Arora, Steven Basart, Eric Tang, Dawn Song, and Jacob Steinhardt. 2021. *Measuring mathematical problem solving with the math dataset*. *Preprint*, arXiv:2103.03874.

Yuxian Jiang, Yafu Li, Guanxu Chen, Dongrui Liu, Yu Cheng, and Jing Shao. 2025. *Rethinking entropy regularization in large reasoning models*. *Preprint*, arXiv:2509.25133.

Feiyang Kang, Michael Kuchnik, Karthik Padthe, Marin Vlastelica, Ruoxi Jia, Carole-Jean Wu, and Newsha Ardalani. 2025. *Quagmires in sft-rl post-training: When high sft scores mislead and what to use instead*. *Preprint*, arXiv:2510.01624.

Ananya Kumar, Aditi Raghunathan, Robbie Jones, Tengyu Ma, and Percy Liang. 2022. *Fine-tuning can distort pretrained features and underperform out-of-distribution*. *Preprint*, arXiv:2202.10054.

Gaotang Li, Ruizhong Qiu, Xiusi Chen, Heng Ji, and Hanghang Tong. 2025. *Beyond log likelihood: Probability-based objectives for supervised fine-tuning across the model capability continuum*. *Preprint*, arXiv:2510.00526.

Mingyang Liu, Gabriele Farina, and Asuman Ozdaglar. 2025a. [Uft: Unifying supervised and reinforcement fine-tuning](#). *Preprint*, arXiv:2505.16984.

Zihan Liu, Zhuolin Yang, Yang Chen, Chankyu Lee, Mohammad Shoeybi, Bryan Catanzaro, and Wei Ping. 2025b. [Acereason-nemotron 1.1: Advancing math and code reasoning through sft and rl synergy](#). *Preprint*, arXiv:2506.13284.

Lu Ma, Hao Liang, Meiyi Qiang, Lexiang Tang, Xiaochen Ma, Zhen Hao Wong, Junbo Niu, Chengyu Shen, Ruming He, Yanhao Li, Bin Cui, and Wentao Zhang. 2025. [Learning what reinforcement learning can't: Interleaved online fine-tuning for hardest questions](#). *Preprint*, arXiv:2506.07527.

Rui Ming, Haoyuan Wu, Shoubo Hu, Zhuolun He, and Bei Yu. 2025. [One-token rollout: Guiding supervised fine-tuning of llms with policy gradient](#). *Preprint*, arXiv:2509.26313.

Nvidia, :, Bo Adler, Niket Agarwal, Ashwath Aithal, Dong H. Anh, Pallab Bhattacharya, Annika Brundyn, Jared Casper, Bryan Catanzaro, Sharon Clay, Jonathan Cohen, Sirshak Das, Ayush Dattagupta, Olivier Delalleau, Leon Derczynski, Yi Dong, Daniel Egert, Ellie Evans, and 64 others. 2024. [Nemotron-4 340b technical report](#). *Preprint*, arXiv:2406.11704.

Long Ouyang, Jeff Wu, Xu Jiang, Diogo Almeida, Carroll L. Wainwright, Pamela Mishkin, Chong Zhang, Sandhini Agarwal, Katarina Slama, Alex Ray, John Schulman, Jacob Hilton, Fraser Kelton, Luke Miller, Maddie Simens, Amanda Askell, Peter Welinder, Paul Christiano, Jan Leike, and Ryan Lowe. 2022. [Training language models to follow instructions with human feedback](#). *Preprint*, arXiv:2203.02155.

Jan Peters, Katharina Mulling, and Yasemin Altun. 2010. Relative entropy policy search. In *Proceedings of the AAAI Conference on Artificial Intelligence*, volume 24, pages 1607–1612.

Rafael Rafailov, Archit Sharma, Eric Mitchell, Stefano Ermon, Christopher D. Manning, and Chelsea Finn. 2024. [Direct preference optimization: Your language model is secretly a reward model](#). *Preprint*, arXiv:2305.18290.

David Rein, Betty Li Hou, Asa Cooper Stickland, Jackson Petty, Richard Yuanzhe Pang, Julien Diranji, Julian Michael, and Samuel R. Bowman. 2023. [Gpqa: A graduate-level google-proof q&a benchmark](#). *Preprint*, arXiv:2311.12022.

Zhiwen Ruan, Yixia Li, He Zhu, Yun Chen, Peng Li, Yang Liu, and Guanhua Chen. 2025. [Enhancing large language model reasoning via selective critical token fine-tuning](#). *Preprint*, arXiv:2510.10974.

John Schulman, Filip Wolski, Prafulla Dhariwal, Alec Radford, and Oleg Klimov. 2017. Proximal policy optimization algorithms. *arXiv preprint arXiv:1707.06347*.

Zhihong Shao, Peiyi Wang, Qihao Zhu, Runxin Xu, Junxiao Song, Xiao Bi, Haowei Zhang, Mingchuan Zhang, Y. K. Li, Y. Wu, and Daya Guo. 2024a. [Deepseekmath: Pushing the limits of mathematical reasoning in open language models](#). *Preprint*, arXiv:2402.03300.

Zhihong Shao, Peiyi Wang, Qihao Zhu, Runxin Xu, Junxiao Song, Xiao Bi, Haowei Zhang, Mingchuan Zhang, YK Li, Yang Wu, and 1 others. 2024b. Deepseekmath: Pushing the limits of mathematical reasoning in open language models. *arXiv preprint arXiv:2402.03300*.

Guangming Sheng, Chi Zhang, Zilingfeng Ye, Xibin Wu, Wang Zhang, Ru Zhang, Yanghua Peng, Haibin Lin, and Chuan Wu. 2024. [Hybridflow: A flexible and efficient rlhf framework](#). *arXiv preprint arXiv: 2409.19256*.

Kimi Team, Yifan Bai, Yiping Bao, Guanduo Chen, Jiahao Chen, Ningxin Chen, Ruijue Chen, Yanru Chen, Yuankun Chen, Yutian Chen, and 1 others. 2025. [Kimi k2: Open agentic intelligence](#). *arXiv preprint arXiv:2507.20534*.

Hugo Touvron, Louis Martin, Kevin Stone, Peter Albert, Amjad Almahairi, Yasmine Babaei, Nikolay Bashlykov, Soumya Batra, Prajwal Bhargava, Shruti Bhosale, Dan Bikel, Lukas Blecher, Cristian Canton Ferrer, Moya Chen, Guillem Cucurull, David Esiobu, Jude Fernandes, Jeremy Fu, Wenyin Fu, and 49 others. 2023. [Llama 2: Open foundation and fine-tuned chat models](#). *Preprint*, arXiv:2307.09288.

Dheeraj Vattikonda, Santhoshi Ravichandran, Emiliano Penalosa, Hadi Nekoei, Megh Thakkar, Thibault Le Sellier de Chezelles, Nicolas Gontier, Miguel Muñoz-Mármol, Sahar Omidi Shayegan, Stefania Raimondo, Xue Liu, Alexandre Drouin, Laurent Charlin, Alexandre Piché, Alexandre Lacoste, and Massimo Caccia. 2025. [How to train your llm web agent: A statistical diagnosis](#). *Preprint*, arXiv:2507.04103.

Shenzi Wang, Le Yu, Chang Gao, Chujie Zheng, Shixuan Liu, Rui Lu, Kai Dang, Xionghui Chen, Jianxin Yang, Zhenru Zhang, Yuqiong Liu, An Yang, Andrew Zhao, Yang Yue, Shiji Song, Bowen Yu, Gao Huang, and Junyang Lin. 2025. [Beyond the 80/20 rule: High-entropy minority tokens drive effective reinforcement learning for llm reasoning](#). *Preprint*, arXiv:2506.01939.

Yubo Wang, Xueguang Ma, Ge Zhang, Yuansheng Ni, Abhranil Chandra, Shiguang Guo, Weiming Ren, Aaran Arulraj, Xuan He, Ziyan Jiang, Tianle Li, Max Ku, Kai Wang, Alex Zhuang, Rongqi Fan, Xiang Yue, and Wenhui Chen. 2024. [Mmlu-pro: A more robust and challenging multi-task language understanding benchmark](#). *Preprint*, arXiv:2406.01574.

Yongliang Wu, Yizhou Zhou, Zhou Ziheng, Yingzhe Peng, Xinyu Ye, Xinting Hu, Wenbo Zhu, Lu Qi, Ming-Hsuan Yang, and Xu Yang. 2025. [On the](#)

generalization of sft: A reinforcement learning perspective with reward rectification. *Preprint*, arXiv:2508.05629.

Jianhao Yan, Yafu Li, Zican Hu, Zhi Wang, Ganqu Cui, Xiaoye Qu, Yu Cheng, and Yue Zhang. 2025. Learning to reason under off-policy guidance. *Preprint*, arXiv:2504.14945.

An Yang, Anfeng Li, Baosong Yang, Beichen Zhang, Binyuan Hui, Bo Zheng, Bowen Yu, Chang Gao, Chengen Huang, Chenxu Lv, Chujie Zheng, Dayiheng Liu, Fan Zhou, Fei Huang, Feng Hu, Hao Ge, Haoran Wei, Huan Lin, Jialong Tang, and 41 others. 2025. Qwen3 technical report. *Preprint*, arXiv:2505.09388.

Qiyi Yu, Zheng Zhang, Ruofei Zhu, Yufeng Yuan, Xiaochen Zuo, Yu Yue, Weinan Dai, Tiantian Fan, Gaohong Liu, Lingjun Liu, Xin Liu, Haibin Lin, Zhiqi Lin, Bole Ma, Guangming Sheng, Yuxuan Tong, Chi Zhang, Mofan Zhang, Wang Zhang, and 16 others. 2025. Dapo: An open-source llm reinforcement learning system at scale. *Preprint*, arXiv:2503.14476.

Shiyue Zhang, Shijie Wu, Ozan Irsoy, Steven Lu, Mohit Bansal, Mark Dredze, and David Rosenberg. 2024. Mixce: Training autoregressive language models by mixing forward and reverse cross-entropies. *Preprint*, arXiv:2305.16958.

Wenhao Zhang, Yuexiang Xie, Yuchang Sun, Yanxi Chen, Guoyin Wang, Yaliang Li, Bolin Ding, and Jingren Zhou. 2025. On-policy rl meets off-policy experts: Harmonizing supervised fine-tuning and reinforcement learning via dynamic weighting. *Preprint*, arXiv:2508.11408.

He Zhu, Junyou Su, Peng Lai, Ren Ma, Wenjia Zhang, Linyi Yang, and Guanhua Chen. 2025a. Anchored supervised fine-tuning. *Preprint*, arXiv:2509.23753.

Wenhong Zhu, Ruobing Xie, Rui Wang, Xingwu Sun, Di Wang, and Pengfei Liu. 2025b. Proximal supervised fine-tuning. *Preprint*, arXiv:2508.17784.

## A Derivation of the Closed-Form Solution for the Global Objective

In this section, we provide the detailed derivation of the closed-form solution for the optimization problem defined in Eq. 3. We seek to find a policy  $\pi$  that maximizes the following KL-regularized reward objective:

$$J_{RL}(\theta) = \mathbb{E}_{x \sim \mathcal{D}, y \sim \pi_\theta} \left[ R(x, y) - \frac{1}{\eta} D_{KL}(\pi_\theta \| \pi_{sft}) \right]$$

Expanding the definition of KL divergence,  $D_{KL}(P \| Q) = \mathbb{E}_{y \sim P} [\log \frac{P(y)}{Q(y)}]$  and using  $R$  instead of  $R(x, y)$ , the objective for a given prompt  $x$  can be rewritten as:

$$\begin{aligned} J_{RL}(\theta) &= \sum_y \pi(y|x) R(x, y) - \frac{1}{\eta} \sum_y \pi(y|x) \log \frac{\pi(y|x)}{\pi_{base}(y|x)} \\ &= \frac{1}{\eta} \sum_y \pi(y|x) \left[ \eta R(x, y) - \log \frac{\pi(y|x)}{\pi_{base}(y|x)} \right] \\ &= \frac{1}{\eta} \sum_y \pi(y|x) \left[ \log \left( \pi_{base}(y|x) e^{\eta R(x, y)} \right) \right. \\ &\quad \left. - \log \pi(y|x) \right]. \end{aligned} \quad (11)$$

To represent the term inside the logarithm as a valid probability distribution, we introduce the partition function  $Z_{base}(x)$ , which acts as a normalization constant:

$$Z_{base}(x) = \sum_y \pi_{base}(y|x) e^{\eta R(x, y)}. \quad (12)$$

Substituting this into the objective, we have:

$$\begin{aligned} J_{RL}(\theta) &= \frac{1}{\eta} \sum_y \pi(y|x) \log \left( \frac{\frac{Z_{base}(x)}{Z_{base}(x)} \pi_{base}(y|x) e^{\eta R(x, y)}}{\pi(y|x)} \right) \\ &= \frac{1}{\eta} \sum_y \pi(y|x) [\log Z_{base}(x) - \\ &\quad \log \frac{\pi(y|x)}{\frac{1}{Z_{base}(x)} \pi_{base}(y|x) e^{\eta R(x, y)}}]. \end{aligned} \quad (13)$$

Since  $\sum_y \pi(y|x) = 1$ , the first term simplifies to  $\frac{1}{\eta} \log Z_{base}(x)$ . Let  $\pi^*(y|x)$  be the Gibbs distribution defined as:

$$\pi^*(y|x) = \frac{1}{Z_{base}(x)} \pi_{base}(y|x) e^{\eta R(x, y)}. \quad (14)$$

The objective  $J(\pi)$  then becomes:

$$J_{RL} = \frac{1}{\eta} \log Z_{base}(x) - \frac{1}{\eta} D_{KL}(\pi(y|x) \| \pi^*(y|x)). \quad (15)$$

Because the KL divergence is always non-negative ( $D_{KL} \geq 0$ ) and achieves its minimum value of zero if and only if the two distributions are identical, the objective  $J(\pi)$  is maximized when  $\pi(y|x) = \pi^*(y|x)$ . Thus, the closed-form solution to the post-training global optimum is:

$$\pi_{global}^*(y|x) = \frac{1}{Z_{base}(x)} \pi_{base}(y|x) e^{\eta R(x, y)}. \quad (16)$$

This completes the derivation.

## B Derivation of Token-Level Alignment

In this section, we provide the detailed derivation bridging the sequence-level optimal policy  $\pi_{sft}^*(y|x)$  (Eq. 7 in the main text) to the token-level training target  $\pi_{sft}^*(y_t|y_{<t}, x)$  utilized in our algorithm.

### B.1 Factorization and Advantage Function

Starting from Eq. 7, the optimal sequence-level policy is defined as:

$$\pi_{sft}^*(y|x) = \frac{1}{Z(x)} \pi_{base}(y|x) e^{\beta R(x, y)},$$

where  $y = (y_1, y_2, \dots, y_T)$ . To derive the token-level policy, we aim to find the conditional distribution  $\pi_{sft}^*(y_t|y_{<t}, x)$ . According to the definition of conditional probability, we have:

$$\pi_{sft}^*(y_t|y_{<t}, x) = \frac{\pi_{sft}^*(y_{\leq t}|x)}{\pi_{sft}^*(y_{<t}|x)}.$$

To evaluate the marginal probability  $\pi_{sft}^*(y_{\leq t}|x)$ , we integrate over all possible future completions  $y'_{>t}$ :

$$\begin{aligned} \pi_{sft}^*(y_{\leq t}|x) &= \sum_{y'_{>t}} \pi_{sft}^*(y_{\leq t}, y'_{>t}|x) \\ &= \frac{1}{Z(x)} \\ &\quad \cdot \sum_{y'_{>t}} \left[ \pi_{base}(y_{\leq t}, y'_{>t}|x) e^{\beta R(x, y_{\leq t}, y'_{>t})} \right] \\ &= \frac{\pi_{base}(y_{\leq t}|x)}{Z(x)} \\ &\quad \cdot \underbrace{\sum_{y'_{>t}} \pi_{base}(y'_{>t}|y_{\leq t}, x) e^{\beta R(x, y_{\leq t}, y'_{>t})}}_{\text{Expected exponentiated reward}} \end{aligned} \quad (17)$$

For simplicity, we define the Soft Q-function  $Q^*(y_{\leq t})$  as the log-expectation of the exponentiated reward:

$$Q^*(y_{\leq t}) = \log \sum_{y_{>t}} \pi_{\text{base}}(y_{>t}|y_{\leq t}, x) e^{\beta R(x, y)}.$$

This definition allows the marginal probability to be expressed compactly as:

$$\pi_{\text{sft}}^*(y_{\leq t}|x) = \frac{1}{Z(x)} \pi_{\text{base}}(y_{\leq t}|x) e^{Q^*(y_{\leq t})}.$$

Substituting this back into the conditional probability identity, we obtain:

$$\begin{aligned} \pi_{\text{sft}}^*(y_t|y_{<t}, x) &= \frac{\pi_{\text{sft}}^*(y_{\leq t}|x)}{\pi_{\text{sft}}^*(y_{<t}|x)} \\ &\propto \frac{\pi_{\text{base}}(y_{\leq t}|x) e^{Q^*(y_{\leq t})}}{\pi_{\text{base}}(y_{<t}|x) e^{Q^*(y_{<t})}}. \end{aligned} \quad (18)$$

Recognizing that  $\frac{\pi_{\text{base}}(y_{\leq t}|x)}{\pi_{\text{base}}(y_{<t}|x)} = \pi_{\text{base}}(y_t|y_{<t}, x)$ , the optimal step-wise policy can be formulated as:

$$\pi_{\text{sft}}^*(y_t|y_{<t}, x) \propto \pi_{\text{base}}(y_t|y_{<t}, x) \cdot e^{A^*(y_t, y_{<t})}, \quad (19)$$

where  $A^*(y_t, y_{<t}) = Q^*(y_{\leq t}) - Q^*(y_{<t})$  denotes the soft advantage function.

## B.2 Approximation under Reward Sparsity

In practice, exact computation of  $Q^*$  involves iterating over all possible future completions, which is intractable. However, we can approximate the advantage landscape by leveraging the ground-truth trajectories  $y^* \in \mathcal{D}$  under two simplifying assumptions:

- 1. Oracle Path Optimality:** The ground-truth token  $y_t^*$  lies on the unique manifold that maximizes the sequence-level reward  $R$ .
- 2. Sparse Recovery:** For any off-policy deviation  $y_t \neq y_t^*$ , the probability of the base model recovering to a high-reward completion is negligible, leading to a sharp decay in  $Q^*(y_{\leq t})$ .

Under these assumptions, the advantage  $A^*$  exhibits a binary structure: it maintains a high value  $\beta$  for the oracle token (preserving the path to  $R_{\max}$ ) and collapses to a baseline (normalized to 0) for incorrect deviations. This yields a computationally efficient first-order approximation:

$$A^*(y_t, y_{<t}) \approx \begin{cases} \beta & \text{if } y_t = y_t^* \\ 0 & \text{if } y_t \neq y_t^* \end{cases} \quad (20)$$

Substituting this approximation back into the policy factorization yields the final training target presented in the main text:

$$\pi_{\text{sft}}^*(y_t|y_{<t}, x) \propto \pi_{\text{base}}(y_t|y_{<t}, x) \cdot e^{\beta \cdot \mathbb{I}(y_t = y_t^*)}. \quad (21)$$

## B.3 Consistency between Sequence and Token Objectives

To verify that the token-level policy  $\pi_{\text{sft}}^*(y_t|y_{<t}, x)$  derived in Eq. 19 is consistent with the sequence-level optimal policy  $\pi_{\text{sft}}^*(y|x) \propto \pi_{\text{base}}(y|x) e^{\beta R(x, y)}$ , we perform a telescoping reconstruction.

According to the chain rule of probability, the joint distribution of a sequence  $y = \{y_1, y_2, \dots, y_L\}$  is:

$$\pi_{\text{sft}}^*(y|x) = \prod_{t=1}^L \pi_{\text{sft}}^*(y_t|y_{<t}, x).$$

Defining  $V(x, y_{\leq t}) = e^{Q^*(y_{\leq t})}$  and substituting the theoretical optimal token-level distribution  $\pi_{\text{sft}}^*(y_t|y_{<t}, x) = \pi_{\text{base}}(y_t|y_{<t}, x) \frac{V(x, y_{\leq t})}{V(x, y_{<t})}$  into the product, we obtain:

$$\pi_{\text{sft}}^*(y|x) = \prod_{t=1}^L \left( \pi_{\text{base}}(y_t|y_{<t}, x) \cdot \frac{V(x, y_{\leq t})}{V(x, y_{<t})} \right).$$

Rearranging the terms, the product of the base model probabilities reconstructs the full sequence-level base distribution, and the value ratios form a telescoping product:

$$\begin{aligned} \pi_{\text{sft}}^*(y|x) &= \pi_{\text{base}}(y|x) \cdot \frac{V(x, y_{\leq 1})}{V(x, y_0)} \\ &\quad \frac{V(x, y_{\leq 2})}{V(x, y_{\leq 1})} \dots \frac{V(x, y_{\leq L})}{V(x, y_{\leq L-1})}, \end{aligned} \quad (22)$$

where  $V(x, y_0)$  is the initial partition function  $Z(x)$ . After cancellation:

$$\pi_{\text{sft}}^*(y|x) = \frac{1}{Z(x)} \pi_{\text{base}}(y|x) V(x, y_{\leq L}).$$

By definition, at the terminal step  $t = L$ , the value function  $V(x, y_{\leq L}) = e^{\beta R(x, y)}$ . Thus, we recover the sequence-level Gibbs distribution:

$$\pi_{\text{sft}}^*(y|x) = \frac{1}{Z(x)} \pi_{\text{base}}(y|x) e^{\beta R(x, y)}.$$

## C Ablation Study: Impact of Uniform Smoothing

While the theoretical framework of GIFT operates on raw base probabilities, practical implementation on base models with weaker priors may encounter numerical underflow where  $p_{\text{ref}}(y_t^*) \approx 0$ . To address this, we employ an optional uniform smoothing step term to advantage adjustment. We calculate the smoothed target logits  $\hat{z}$  as:

$$\hat{z}_{t,k} = \log \left( (1 - \lambda)p_{\text{ref}}(k) + \frac{\lambda}{|\mathcal{V}|} \right) + \beta \cdot \mathbb{I}(k = y_t^*) \quad (23)$$

where  $\lambda$  is the smoothing coefficient,  $|\mathcal{V}|$  denotes the vocabulary size. This operation ensures finite log-probabilities and prevents the model from failing to fit tokens with vanishingly small priors. In practice, we set  $\lambda = 0.01$ .

In this section, we test the impact of the smoothing term across models. As illustrated in Figure 4, the smoothing term becomes particularly critical when the base model lacks strong intrinsic priors. For Llama-3.1-8B, which exhibits a relatively weaker reasoning prior, smoothing prevents numerical divergence caused by vanishing probabilities, yielding a significant performance gain (e.g., 28.94% vs. 26.09% at  $\beta = 10$ ). Conversely, for Qwen2.5-7B, where the base distribution is better calibrated, the smoothing term is largely redundant and results in a marginal performance drop (52.43% peak for unsmoothed) due to unnecessary noise injection. These results indicate that while smoothing is less critical for models with strong priors, it ensures the robustness and training stability of GIFT across diverse architectures.

## D Training Dynamics.

We report the accuracy on mathematical reasoning benchmarks during the RL training in Figure 5. GIFT initialization demonstrates superior sample efficiency and asymptotic performance compared to standard SFT initialization. On Llama-3.1-8B, GIFT maintains a consistent performance advantage over the SFT baseline out the entire optimization process. Meanwhile, on Qwen2.5-7B, we observe a crossover phenomenon: although GIFT begins with slightly lower performance, it rapidly overtakes the SFT baseline within the first 25% steps. This trajectory indicates that GIFT effectively avoids the premature convergence often induced by rigid supervision, trading off negligible

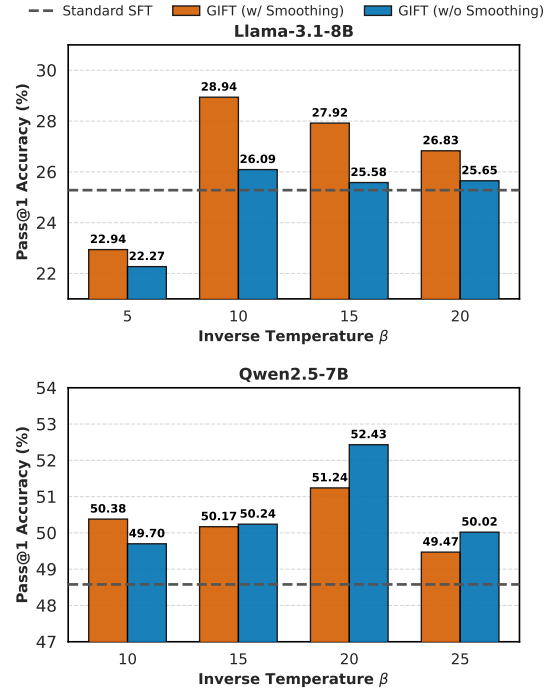


Figure 4: Ablation study of the uniform distribution smoothing term.

initial exploitation for substantially greater exploration potential and superior long-term gains.

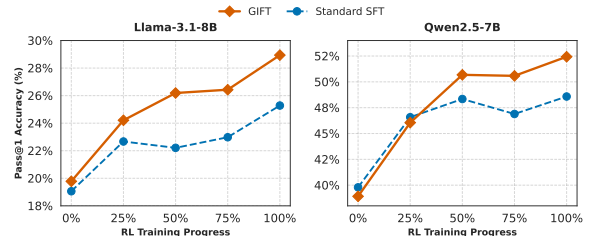


Figure 5: Average pass@1 accuracy across the RL training progress.

## E Implementation Details

In this section, we provide the detailed experimental configuration to facilitate reproducibility. All experiments are conducted using the VeRL framework (Sheng et al., 2024) on a cluster of  $8 \times$  NVIDIA H200 GPUs.

### E.1 Supervised Fine-Tuning

**Training Configuration.** We optimize the base models using the AdamW optimizer with  $\beta_1 = 0.9$ ,  $\beta_2 = 0.95$ , and a weight decay of 0.01. The global batch size is set to 128. We employ a constant learning rate of  $1 \times 10^{-5}$  with no warmup steps. To accommodate long chain-of-thought reasoning,

we set the maximum sequence length to 8,192 tokens. Following standard practices for generative fine-tuning, we apply right-side truncation for input sequences. For Llama-3.1-8B, a uniform label smoothing term is applied to mitigate instability. We use the default configuration for other baselines.

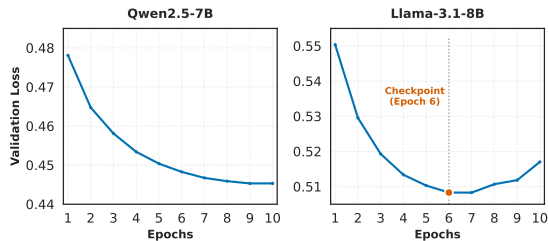


Figure 6: **Validation loss across the SFT stage.** While Qwen2.5-7B shows continuous improvement, Llama-3.1-8B exhibits overfitting after the 6th epoch.

**RL Initialization Protocol.** To identify the optimal initialization for the RL stage, we closely monitored the validation loss of the SFT models on a held-out validation set. As illustrated in Figure 6, while Qwen2.5-7B exhibits a continuously decreasing loss, Llama-3.1-8B reaches a minimum at the 6th epoch before the loss begins to rise, signaling potential overfitting. Drawing on recent findings (Kang et al., 2025) that correlate SFT validation loss with downstream RL performance, we prioritize the generalization capability of the base policy. Consequently, to balance training efficiency with performance and to maintain a standardized protocol across backbones, we uniformly select the checkpoint from the 6th epoch as the initialization for the subsequent RL stage. For the direct SFT baseline, to ensure fairness, we trained on a training set containing both SFT and RL data with the same data size configuration.

## E.2 Reinforcement Learning

Following SFT, we apply the Group Relative Policy Optimization (GRPO) algorithm (Shao et al., 2024b) to refine the policy. During the exploration phase, we sample  $G = 8$  outputs per prompt with a temperature of  $T = 1.0$  to encourage diversity. The policy is optimized using a constant learning rate of  $1 \times 10^{-6}$  and a global batch size of 128 (mini-batch size of 64). We set the clip ratio to 0.2, disable advantage normalization (norm\_adv\_by\_std=False), and set the KL coefficient to 0.0, relying implicitly on the group-relative advantage for regularization. To prevent reward hacking, we restrict training to 1 epoch.

## E.3 Evaluation and Reward Mechanism

**Evaluation.** We report the average pass@1 accuracy across four runs for all benchmarks, except for Llama3.1-8b on AIME24/25, where we report pass@32 due to limited model ability. We merge FSDP checkpoints and utilize vLLM for high-throughput inference with a temperature of  $T = 0.6$  and a max token limit of 8,192.

**Reward Function.** We employ a cascaded binary reward function that sequentially utilizes OpenMathInstruct extraction rules and the MathVerify parser. To ensure stability, the verification process is guarded by a 10-second thread-based timeout, assigning a reward of 1.0 if either method validates the solution against the ground truth.

## F Use of AI Assistants

We utilized AI assistants exclusively for grammatical polishing and LaTeX formatting assistance.